

Response surface optimised photocatalytic degradation and quantitation of repurposed COVID-19 antibiotic pollutants in wastewaters; towards greenness and whiteness perspectives

Heba T. Elbalkiny^A, Ola M. El-Borady^B, Sarah S. Saleh^{A,*}  and Christine M. El-Maraghy^A

Environmental context. The consumption of repurposed antibiotics increased due to the management of COVID-19, which in turn led to their increased presence in wastewater and potential environmental effects. This change has created a greater need for their analysis and treatment in different environmental water. This work presents a safe, low-cost method for analysing and treating water samples to ensure their suitability for human and animal use.

For full list of author affiliations and declarations see end of paper

***Correspondence to:**

Sarah S. Saleh
 Analytical Chemistry Department, Faculty of Pharmacy, October University for Modern Sciences and Arts (MSA), 11787 6th October City, Cairo, Egypt
 Email: drsarahsalah@gmail.com

Handling Editor:

Graeme Batley

Received: 19 September 2023

Accepted: 2 December 2023

Published: 20 December 2023

Cite this:

Elbalkiny HT *et al.* (2023)
Environmental Chemistry
 20(6), 268–280. doi:[10.1071/EN23092](https://doi.org/10.1071/EN23092)

© 2023 The Author(s) (or their employer(s)). Published by CSIRO Publishing.

This is an open access article distributed under the Creative Commons Attribution 4.0 International License ([CC BY](https://creativecommons.org/licenses/by/4.0/))

OPEN ACCESS

ABSTRACT

Rationale. Certain antibiotics have been repurposed for the management of infected COVID-19 cases, because of their possible effect against the virus, and treatment of co-existing bacterial infection. The consumption of these antibiotics leads to their access to sewage, industrial and hospital effluents, then to environmental waters. This creates a need for the routine analysis and treatment of water resources. **Methodology.** Detection and quantitation of three repurposed antibiotics: levofloxacin (LEVO), azithromycin (AZI) and ceftriaxone (CEF) were studied in different water samples using LC-MS/MS methods employing a C₁₈ column and a mobile phase consisting of 80% acetonitrile/20% (0.1% formic acid in water) after solid phase extraction on Oasis HLB Prime cartridges. Real water samples were treated with synthesised graphitic carbon nitride (g-C₃N₄) to remove the three types of antibiotics from contaminated water under experimental conditions optimised by response surface methodology, using Box–Behnken experimental design. **Results.** The analytical method was validated in the concentration range of 10–5000 ng mL⁻¹ for the three drugs. The removal percentages were found to be 92.55, 98.48 and 99.10% for LEVO, AZI and CEF, respectively, using synthesised g-C₃N₄. **Discussion.** The analytical method was used for the estimation of the three cited drugs before and after their removal. The method was assessed using ComplexGAPI as a greenness tool and the RGB I2 algorithm as a whiteness model. The method was applied for the analysis and treatment of real water samples before and after their treatment. It proved to be simple, low-cost and environmentally sustainable.

Keywords: azithromycin, Box–Behnken, ceftriaxone, ComplexGAPI, g-C₃N₄, levofloxacin, liquid chromatography, mass spectrometry.

Introduction

In the year 2019, the world was exposed to the first pandemic, COVID-19, and the number of infected cases exceeded 400 million by the end of 2022 (WHO Coronavirus (COVID-19) 2023). To face this plight, several approaches were adopted, such as preparing effective vaccines and inventing new molecules to treat the virus. Unfortunately, these approaches went on for some time with no immediate solution. Meanwhile, certain antibiotics were repurposed for the management of infected cases, because of their possible effect against the virus, and treatment of co-existing bacterial infection. These classes of antibiotics included fluoroquinolones, macrolides and cephalosporins (Yacouba *et al.* 2021; Thapa *et al.* 2022). Concerns about repurposed antibiotic consumption increased; accordingly, they found their way through sewage, industrial and hospital effluents into receiving environment waters (Hayden *et al.* 2022; Wang *et al.* 2022). There is an environmental risk of bioaccumulation

of antibiotics to levels which would cause bacterial resistance, endocrine disturbance and genotoxic effects (Elbalkiny *et al.* 2020; Elbalkiny and Yehia 2022; Tantawy *et al.* 2023).

The selected antibiotics for this study were azithromycin (AZI), levofloxacin (LEVO) and ceftriaxone (CEF). AZI belongs to the checklist of substances to be monitored throughout the European Union in the field of water policy (Directive 2015/495/EC of 20 March 2015) as it poses a significant risk to the aquatic environment (Vella 2015). It was repurposed for patients with COVID-19 at the beginning of the pandemic due to its antiviral and immunomodulatory activity; however, AZI's role in COVID-19 is still unclear (Parnham *et al.* 2014). LEVO is the first-line therapeutic agent for the management of respiratory tract infections due to its safety profile and high concentration in the lungs (Karampela and Dalamaga 2020). It continues to appear in the aquatic environment because of its insufficient metabolism in human bodies (Felis *et al.* 2020). CEF is prescribed to treat COVID-19 patients because of the possible complications of bacterial superinfections which have been previously reported in the case of other viral respiratory infections (Giacomelli *et al.* 2021). It accumulates in water and causes ecological, environmental and health issues (Guo *et al.* 2015).

In the last few years, LEVO, AZI and CEF have been analysed either separately or with other antibiotics, in different types of wastewater samples by applying liquid chromatographic methods coupled with solid phase extraction (SPE) (Diwan *et al.* 2013; Oprüş *et al.* 2013; Yu *et al.* 2016; Aydin *et al.* 2019; Younes *et al.* 2019; Serra-Compte *et al.* 2021; Sharma *et al.* 2022). AZI and LEVO were simultaneously detected in wastewater samples after SPE using liquid chromatography (LC) analysis (Yasojima *et al.* 2006; Golovko *et al.* 2014). The three drugs (LEVO, AZI and CEF) were quantified among other antimicrobials in water and livestock excreta using liquid chromatography with tandem mass spectrometry (LC-MS/MS) (Gao *et al.* 2016). Their presence in water could lead to the development of antibiotic resistance. As such there is great interest in their elimination. Unfortunately conventional methods are not successful for their removal in wastewater, therefore advanced methods are required, such as adsorption or an advanced oxidation process.

Different advanced methods have been reported for the removal of antibiotics from water by an adsorption process: for LEVO (Ullah *et al.* 2019; Li *et al.* 2020b; Gopal *et al.* 2022; El-Maraghy *et al.* 2023), AZI (Balarak *et al.* 2021; Upoma *et al.* 2022; Ameen *et al.* 2023) and CEF (Karungamye *et al.* 2022; Mohammadi Nezhad *et al.* 2023), and biological treatments (Tian *et al.* 2019; de Ilurdoz *et al.* 2022). The application of these methods is limited due to their high cost, low degradation efficiency, second-pollution and complicated technology (Jiang *et al.* 2012). Photocatalytic degradation is one of the most promising advanced oxidation processes (AOPs) that depends on the oxidation of the pollutants through the production of highly reactive radicals formed upon exposure of a photocatalyst to a UV or a solar/visible

light source yielding, by mineralisation, less harmful products such as water, carbon dioxide and intermediates (Dewil *et al.* 2017). Photocatalytic degradation has the advantages of being eco-friendly, simple, economic, nontoxic, highly stable and possesses excellent degradation efficiency (Jiang *et al.* 2012). Literature reviews have revealed the use of nanoparticles as photocatalysts for the removal of the three studied antibiotics using different metal nanocomposites such as silver, zinc, iron and titanium oxide nanoparticles (Shokri *et al.* 2016; Naraginti *et al.* 2019; Sayadi *et al.* 2019; El-Maraghy *et al.* 2020; Hashemi *et al.* 2020; Mehrdoost *et al.* 2021; Salei and Nezamzadeh-Ejhieh 2022), graphene composites (Li *et al.* 2020a), and functionalised iron magnetic nanocatalysts (Shokri *et al.* 2016; Naraginti *et al.* 2019; Sayadi *et al.* 2019; El-Maraghy *et al.* 2020; Li *et al.* 2020a; Goulart *et al.* 2021; Gulen *et al.* 2021; Guo *et al.* 2021; Hu *et al.* 2021; Mehrdoost *et al.* 2021; Shen *et al.* 2021; Zhang *et al.* 2021; Salei and Nezamzadeh-Ejhieh 2022; Abdullah *et al.* 2023), as shown in Supplementary Table S1.

One of the photocatalysts that has lately experienced a renaissance as a highly active metal-free photocatalyst is graphitic carbon nitride ($g\text{-C}_3\text{N}_4$), which renders materials nontoxic and biocompatible (Zhao *et al.* 2018; AttariKhasraghi *et al.* 2021; John and Thomas 2022). It displays significant blue photoluminescence between 430 and 550 nm at room temperature with onset of the bandgap adsorption at around 420 nm. Moreover, $g\text{-C}_3\text{N}_4$ has bandgap of 2.7 eV which make it suitable as a visible light-active photo-responsive photocatalyst with a conductive band of -1.1 eV and valence band of $+1.6$ eV, respectively (Ong *et al.* 2016). The $\text{OH}\cdot$ radical dot and holes are the two main reactive species in $g\text{-C}_3\text{N}_4$ that are responsible for the photocatalytic degradation of the studied drugs (Raizada *et al.* 2020). So, it is considered an economic, green and safe photocatalyst that requires only solar radiation as a driving force to conduct the catalytic reaction. Therefore, $g\text{-C}_3\text{N}_4$ has been used as a photocatalyst for the degradation of organic pollutants (Alias *et al.* 2020; AttariKhasraghi *et al.* 2021; John and Thomas 2022).

This study aimed to detect and quantify the repurposed antibiotics LEVO, AZI and CEF in different water samples coinciding with their reported treatment of COVID-19 infections using LC-MS/MS detection. The water samples were extracted using SPE and treated using the synthesised green and safe photocatalyst $g\text{-C}_3\text{N}_4$ under experimental conditions optimised by response surface methodology. The whole process is assessed in terms of Green Analytical Chemistry (GAC) and White Analytical Chemistry (WAC).

Experimental

Analysis methodology

Instrument and reagents

The analysis was performed using a Shimadzu LC-MS/MS with a pump (model LC-20AD). The detection was performed

using a triple quadrupole mass spectrometer (API 4000) equipped with an electrospray ionisation (ESI) source using multiple reaction monitoring (MRM) in positive ion mode. An autosampler was used with a sampling speed of $15 \mu\text{L s}^{-1}$ (Shimadzu SIL20A) and a pump (Shimadzu LC20AD). The data acquisitions were performed using Analyst 1.6.3 software. Oasis HLB Prime cartridges (500 mg/6 mL, Waters, MA, USA) were used for sample treatment.

For characterisation of $g\text{-C}_3\text{N}_4$, a JEOL JEM-2010 transmission electron microscope, a Shimadzu UV-2450 spectrophotometer, a Malvern Zetasizer Nano ZS90 analyser, a Shimadzu RF5301PC spectrofluorometer, an FTIR spectrophotometer (JASCO spectrometer), a Shimadzu XRD 6100 diffractometer, a Jeol model JSM-IT100 scanning electron microscope, and a Quantachrome TouchWin™ (ver. 1.2) surface analyser were used.

A reference standard of LEVO (99.54 ± 0.67) was kindly supplied by the Sanofi pharmaceutical company (Egypt). A reference standard of ceftriaxone sodium (99.58 ± 0.56) was kindly supplied by EIPICO pharmaceutical company (Egypt). Methanol, acetonitrile (HPLC grade), formic acid, melamine ($\geq 99\%$), a reference standard of azithromycin dehydrate (99.78 ± 0.73), and erythromycin as an internal standard (IS) were purchased from Sigma–Aldrich, USA. Sodium hydroxide and hydrochloric acid (33%) were obtained from ADWIC (Egypt). The purity of the reference standards was checked using the official British Pharmacopoeia (BP) methods (British Pharmacopoeia Commission 2013).

Chromatographic and mass conditions

The separation and identification were performed using an Agilent C_{18} column ($4.6 \text{ mm} \times 50 \text{ mm}$, $4.6 \mu\text{m}$ particle size). The mobile phase consisted of 80% acetonitrile/20% (0.1% formic acid in water) in isocratic elution mode delivered at a flow rate of 0.8 mL min^{-1} . The column temperature was set at 30°C and the amount of sample injected was $5 \mu\text{L}$. A mass spectrometer (API 4000) equipped with a triple quadrupole was used and the detection was achieved using positive ion electrospray ionisation (ESI+), with air as a nebuliser gas and nitrogen as an auxiliary curtain and collision gas. The gas temperature was set at 300°C . The MRM transitions for LEVO, AZI, CEF and erythromycin (IS), and mass spectrometric parameters, are listed in Table 1.

Construction of calibration curves and method validation

Stock standard solutions of LEVO, AZI, CEF and erythromycin (IS) were prepared in methanol to a concentration of $100 \mu\text{g mL}^{-1}$. Freshly prepared working solutions for the three drugs were prepared by dilution of the stock solution using the same solvent. The calibration curves for the three drugs were prepared using concentrations of $10\text{--}500 \text{ ng mL}^{-1}$ in triplicate for each drug. A calibration curve was plotted for each drug relating the prepared concentrations versus the peak area ratio of the corresponding drug to that of the IS. The three calibration curves were plotted, and regression equations were computed. Validation of the analytical method was performed as per ICH guidelines including the parameters of linearity, range, accuracy and precision, specificity, limit of quantification (LOQ) and limit of detection (LOD) (ICH Harmonisation Tripartite Guideline 2005).

Water sample preparation and preconcentration

In 250-mL amber glass bottles, 200 mL of water samples were collected from different locations and stored at -15°C for 10 days till extraction and analysis. These water samples were filtered through Whatman No. 41 and $0.7\text{-}\mu\text{m}$ filters prior to the preconcentration process, at the original pH (7–7.5) using an Oasis HLB Prime cartridge (500 mg/6 mL). Loading the cartridges was done at a flow rate of 1 mL min^{-1} using ultra-water samples for a sufficient contact time to allow targeted antibiotics to adsorb on the sorbent material. The sorbent was washed with 10 mL of water and then dried under vacuum and eluted with methanol ($3 \times 10 \text{ mL}$). The solvent was evaporated under nitrogen and the water samples were analysed according to the chromatographic conditions.

Synthesis and characterisation of graphitic carbon nitride ($g\text{-C}_3\text{N}_4$)

Synthesis of $g\text{-C}_3\text{N}_4$

The pristine $g\text{-C}_3\text{N}_4$ powder was synthesised in a one-step process by thermally polymerising melamine (Svoboda et al. 2019) following the literature procedure with a simple modification: 5 g of melamine was weighed and placed in a porcelain crucible, which was then covered and heated in a muffle furnace for 4 h in an air atmosphere at 550°C with a heating rate of 2°C min . The resulting, yellow-coloured

Table 1. The selected LC-MS/MS parameters for the quantification of LEVO, AZI and CEF.

	Precursor (Da)	Product (Da)	Dwell (ms)	Cone (V)	Collision energy (V)	Ion mode
LEVO	362.1	318.3	300.0	25.0	25.0	ESI+
AZI	749.6	83.0	300.0	30.0	25.0	ESI+
CEF	555.2	396.0	300.0	30.0	20.0	ESI+
Erythromycin (IS)	734.6	158.0	300.0	30.0	25.0	ESI+

product was kept at room temperature for later investigations and use.

Characterisation of g-C₃N₄

The morphological characteristics were analysed using a transmission electron microscope, operated at an accelerating voltage of 200 kV, and included a Gatan digital camera (Model Erlangshen ES500). A Zeta sizer set to 25°C was used to determine the zeta-potential. The optical features of the solid sample were recorded using a spectrophotometer with 1 cm quartz cells. The g-C₃N₄ photoluminescence (PL) emission spectra were captured utilising a spectrofluorometer. The structural information and functional groups were identified using an FTIR spectrophotometer in the 4000–400 cm⁻¹ range. X-Ray diffraction data were collected using a diffractometer with CuKα1 radiation ($k = 1.54056 \text{ \AA}$), a 2θ range of 10–80, an operating data voltage of 40 kV, and a current of 30 mA. Energy-dispersive X-ray spectrometry (EDX) was utilised using a scanning electron microscope (SEM). The BET surface area of the sample was calculated employing a multipoint Brunauer–Emmett–Teller (BET) method using adsorption data relative pressure (P/P_0) in the range of 0.05–0.9. The particle pore size distribution was measured by the Barrett–Joyner–Halenda (BJH) method using adsorption data, both methods were performed on a Quantachrome Nova instrument running TouchWin™ software (ver. 1.2).

Photocatalytic degradation experiment

Screening and optimisation of photocatalytic degradation

The treatment of the studied antibiotics was undertaken using synthesised g-C₃N₄ nanosheets under a LED lamp (35 W) which produced visible light irradiation. Screening experiments were performed under variable conditions including pH ranges, initial concentrations of the three drugs, dose of g-C₃N₄, agitation rate, and time intervals in the dark to obtain an adsorption–desorption equilibrium, where one condition was changed while the others were kept constant. Two millilitres of each suspension was taken and centrifuged to remove the photocatalyst powders before measurement. The sample was analysed using the developed LC-MS/MS procedure. The screening experiments revealed the factors that will be included in the experimental design.

Box–Behnken experimental design (BBD), three-levels and three-factors, was employed for assigning the optimum conditions for maximising the removal of the three selected antibiotics, LEVO, AZI and CEF as dependent variables, against the dose of g-C₃N₄ (0.2–1.0 g L⁻¹), pH (5–9) and time (30–90 min) as independent variables. Each variable was represented in three levels, high (+1), medium (0) and low (–1). Fifteen experimental points were performed including replications of the central points in randomised

experimental order, as shown in Supplementary Table S2. ANOVA data analysis was performed to determine the lack of fit, and evaluate other parameters including the effects of quadratic, linear and variables' interaction, where the model was verified by response surface methodology (RSM).

Application to synthetic and real water samples

Optimum experimental conditions were applied to three types of water. The first type of water sample was a laboratory distilled water spiked with equal amounts of the three cited pharmaceuticals (500 ng mL⁻¹). The second one was a real water sample free from pharmaceutical pollutants (clean real water) and spiked with equal amounts of the three cited pharmaceuticals (500 ng mL⁻¹). The third were contaminated real water samples collected from the Nile River and industrial effluents collected from two cities named 6th of October and 10th of Ramadan. This approach allowed monitoring the degradation under realistic working conditions compared to the laboratory experiments.

Results and discussion

LC-MS/MS quantitation of water pollutants

LC-MS/MS analysis and validation sheet

Several mobile phase components with different ratios (methanol, acetonitrile, water and acidified water with formic acid) were trialled to elute symmetrical peaks with accepted tailing factors for the three drugs and IS. A C₁₈ column and a mobile phase consisting of 80% acetonitrile/20% (0.1% formic acid in water) in isocratic elution mode at a flow rate of 0.8 mL min⁻¹ gave optimum results as formic acid helped in the positive ionisation of the drugs. Regarding the mass spectrometric detector, the positive ion mode was selected for MRM analysis where the parent ions were selected at m/z 362.12 > 318.3 for LEVO, 555.2 > 396 for CEF, 749.61 > 83.0 for AZI and 734.55 > 158 for IS, as shown in Fig. 1a, b.

The validation parameters are presented in Table 2. The linearity range was 10–5000 ng mL⁻¹ for AZI, CEF and LEVO as shown in Supplementary Fig. S1. The accuracy of the method was confirmed by calculating the recovery % of each drug using the corresponding regression equations. The inter- and intra-day precision scored %RSD < 2 units. The method was specific as it could determine the three drugs simultaneously without interference in the laboratory prepared mixtures. The LOD of the drugs was ~3.5 ng mL⁻¹ and LOQ was ~9 ng mL⁻¹, which prove the high sensitivity of the method.

Analysis of spiked and real water samples

Oasis Prime HLB cartridges are preferred over HLB cartridges for SPE because they eliminate the conditioning step, and thus reduce solvent consumption and sample

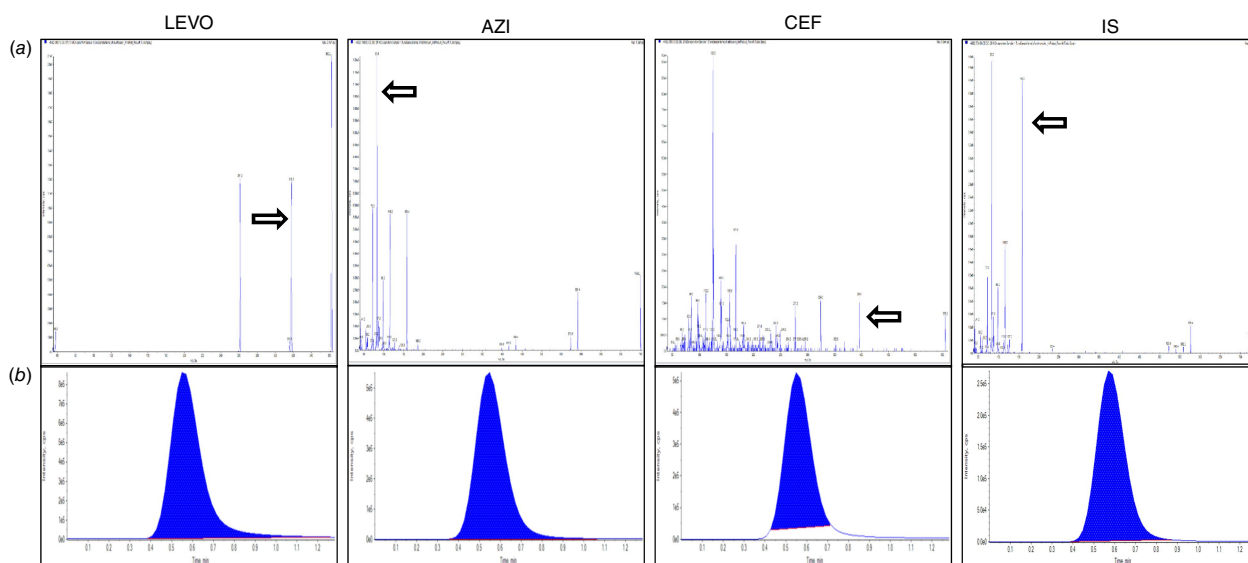


Fig. 1. (a) Product ion spectra of $[M + H]^+$ of the positive ion ESI-MS/MS spectra: LEVO 362.12 > 318.3 (m/z), AZI 749.61 > 83.0 (m/z), CEF 555.2 > 396 (m/z) and IS 734.55 > 158 (m/z); (b) multiple reaction monitoring (MRM) chromatograms of the three drugs and IS.

Table 2. Validation sheet for the proposed LC-MS/MS method for the quantification of LEVO, AZI and CEF.

Parameter	LEVO	AZI	CEF	
Linearity range (ng mL^{-1})	10–5000			
Correlation coefficient (r)	0.997	0.991	0.9996	
Slope	0.0009	0.0006	0.0004	
Intercept	-0.0114	0.0676	-0.01	
s.d. of residuals	0.099	0.110	0.018	
LOD ^A (ng mL^{-1})	6.04	6.6	6.34	
LOQ ^A (ng mL^{-1})	9.75	9.63	9.91	
Accuracy ^B (Recovery % \pm s.d.)	99.83 \pm 1.21	99.37 \pm 1.25	99.0 \pm 0.81	
Precision ^C (%RSD)	Intra-day	1.32	0.65	1.37
	Inter-day	1.54	1.43	1.92

^ALOD = (s.d. of the response/slope) \times 3.3; LOQ = (s.d. of the response/slope) \times 10.

^BThe average of five experiments.

^CThe average of nine experiments.

preparation time. They were also reported to have higher extraction recoveries (40%) than HLB cartridges that are reported to be commonly used for sample preconcentration of pharmaceuticals in complex environmental matrices (Elbalkiny *et al.* 2019; Yehia *et al.* 2019), even though the sorbent is the same in both cartridges (*N*-vinylpyrrolidone and divinylbenzene copolymer). As a result, Oasis Prime HLB cartridges at the original sample pH were chosen as they enabled a greener and better recovery of the selected drugs using a single solvent elution with pure methanol after spiking all water samples with 100 ng of each drug standard. The analysis of laboratory-spiked distilled water yielded the

recovery of cartridges, and it was found to be 86.3, 83.8 and 89.1% for LEVO, AZI and CEF, respectively. The contaminated real water samples showed the presence of one or two of the cited drugs in each sample as shown in Table 3, while the clean real samples didn't show any traces of the three drugs.

Characterisation analysis of g-C₃N₄

A typical transmission electron microscopy (TEM) image demonstrates the formation of mesoporous g-C₃N₄ as loose agglomerates with an irregular shape (Fig. 2a). The images

Table 3. LEVO, AZI, and CEF in real water samples using LC-MS/MS method.

Real water	Concentration before photodegradation			Concentration after photodegradation			Photodegradation (%)		
	LEVO	AZI	CEF	LEVO	AZI	CEF	LEVO	AZI	CEF
Sample ^A 1	n.d. ^B	n.d. ^B	187.5 ^C	–	–	14.8 ^C	–	–	92.1
Sample ^A 2	n.d. ^B	458.1 ^C	1109.9 ^C	–	27.48 ^C	33.3 ^C	–	94.0	97.0
Sample ^A 3	247.9 ^C	n.d. ^B	n.d. ^B	22.1 ^C	–	–	91.1	–	–

^ASample 1: Nile River, sample 2: industrial effluents collected from 6th of October city, and sample 3: industrial effluents collected from 10th of Ramadan city.

^BNot detected.

^CConcentration in ng/mL calculated using the proposed LC-MS/MS method.

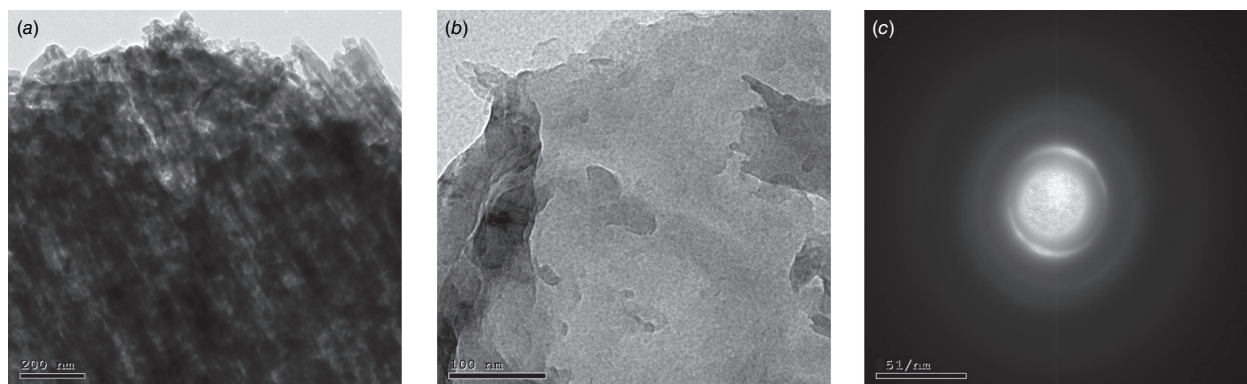


Fig. 2. (a, b) TEM images of the synthesised $g\text{-C}_3\text{N}_4$ at different magnification scales. (c) The SAED pattern of $g\text{-C}_3\text{N}_4$.

also show a layered and plate-like and a worm-like porous structure (Fig. 2b) due to the substantial amounts of NH_3 that may be released from the precursors which is attributed to an intrinsic catalytic property (Zhu *et al.* 2015). Furthermore, the selected area electron diffraction (SAED) pattern showed diffraction rings corresponding to 201 and 220 crystal planes (Fig. 2c) (Sun *et al.* 2022). Energy-dispersive X-ray spectroscopy (EDX) revealed the purity of the prepared sample and existence of all the anticipated elements in the photocatalyst, carbon (29.3%) and nitrogen (71.1%), as shown in Supplementary Fig. S2. The zeta (ζ) potential of $g\text{-C}_3\text{N}_4$ showed a value of -36.06 mV (Supplementary Fig. S3a), which reflects a high stability (El-Borady *et al.* 2021). The X-ray diffraction (XRD) pattern in Supplementary Fig. S3b displays a characteristic intense peak at a 2θ value of 27.7° (Zhu *et al.* 2015) which is characteristic of $g\text{-C}_3\text{N}_4$ (Liu *et al.* 2020). The surface features and adsorption–desorption isotherms were studied using BET and BJT as shown in Supplementary Table S3. As seen in Supplementary Fig. S3c, the adsorption–desorption isotherms were of type IV as a H3 hysteresis loop, implying the mesoporous nature of $g\text{-C}_3\text{N}_4$ which is consistent with its TEM images. The current BET surface area value is significantly greater than that previously prepared using melamine as a precursor (Yan 2012; Zhu *et al.* 2015). This increased surface area could be attributed to oxidation and exfoliation of $g\text{-C}_3\text{N}_4$, which are brought on by prolonged calcination and result in a more active catalytic surface, which is considered

the key to the superior photocatalytic potential of the prepared $g\text{-C}_3\text{N}_4$. The structural and functional group information was demonstrated by FTIR analysis of both the melamine and the prepared $g\text{-C}_3\text{N}_4$, as in Supplementary Fig. S4, showing their characteristic spectra. The optical properties of the $g\text{-C}_3\text{N}_4$ were acquired by measuring its UV-Vis diffuse reflectance (DRS) (Zhang *et al.* 2016). Furthermore, the photoluminescence (PL) spectroscopy explained the photocatalytic potential as shown in Fig. 3. The PL spectrum (excitation at 325 nm) showed an emission peak around 443 nm that was ascribed to $n\text{-}\pi^*$ electronic transitions that included the lone pairs of the nitrogen atoms in $g\text{-C}_3\text{N}_4$ (Svoboda *et al.* 2019).

Photocatalytic degradation using $g\text{-C}_3\text{N}_4$

Photodegradation mechanism

Based on the above characterisation results, the bandgap of $g\text{-C}_3\text{N}_4$ is relatively narrow, so it can generate electron–hole pairs under visible light irradiation. The photoexcited electrons in the conduction band (CB) of $g\text{-C}_3\text{N}_4$ can react with O_2 in air to produce active superoxide radicals (O_2^-), where this generated species can react with electrons to form H_2O_2 . H_2O_2 then reacts with electrons to form hydroxyl radicals (OH). O_2^- , OH and H_2O_2 generated by $g\text{-C}_3\text{N}_4$ are involved in converting antibiotic pollutants into carbon dioxide and water (Dong *et al.* 2022), as shown in Supplementary Fig. S5.

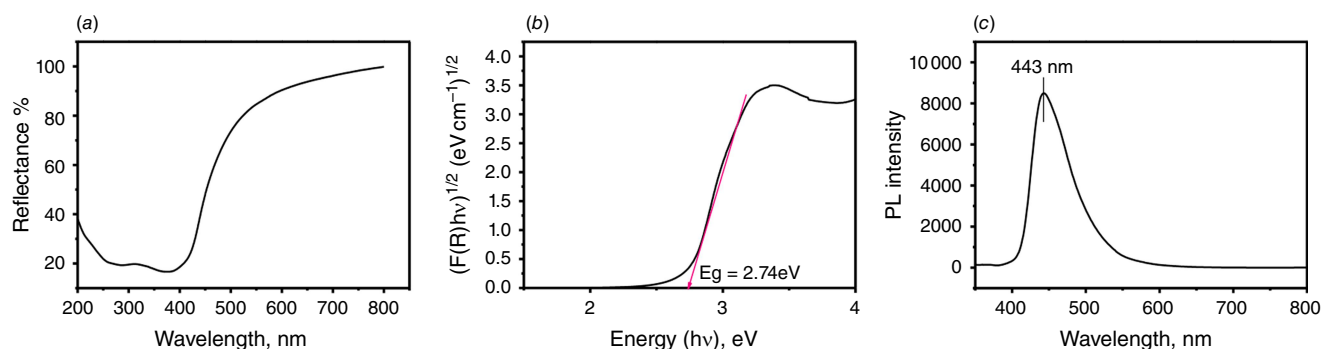


Fig. 3. UV-Vis diffuse reflectance spectra of g-C₃N₄ (a), its band gap calculation (b), and its photoluminescence emission spectrum at an emission peak of 443 nm (c).

Table 4. ANOVA and fit statistics of the BBD model.

Parameters	Removal % LEVO	Removal % AZI	Removal % CEF
Model <i>F</i> value	35.7	26.4	30.5
Model <i>P</i> value	0.0005	0.0011	0.0008
<i>R</i> ²	0.9847	0.9794	0.9821
<i>R</i> ² (adjusted)	0.9571	0.9422	0.9498
<i>R</i> ² (predicted)	0.8805	0.8601	0.8994
Adequate precision	16.4936	14.0111	15.1717

Screening experiment

The performance of the photocatalytic activity of g-C₃N₄ depends on different variables. Different pH ranges, initial concentrations of the three drugs, dose of g-C₃N₄, agitation rate and time intervals were studied. After the exploratory runs, it was found that the initial concentration of the studied antibiotics and the agitation rate had insignificant effects on the degradation rate. Meanwhile, the pH of the solution, dose of g-C₃N₄, and time intervals played a remarkable role in the photocatalytic reactions. As such, these three variables were included in the optimisation study that was designed via response surface methodology.

Response surface modelling and analysis of variance

The quadratic statistical models were suggested with the highest order polynomial based on the experimental design results and statistical analysis performed on the three responses (highest *F* value and lowest *P* value). The model results obtained by experimental design are shown in Eqns 1–3:

$$\begin{aligned} \text{Removal \% of LEVO} = & + 88.67 - 7.13A + 2.75B \\ & + 10.38C + 3.00AB - 5.75AC \\ & + 7.00BC - 34.96A^2 - 13.71B^2 \\ & - 7.46C^2, \end{aligned} \quad (1)$$

$$\begin{aligned} \text{Removal \% of AZI} = & + 90.33 - 7.50A + 2.12B \\ & + 11.38C + 3.75AB - 6.25AC \\ & + 6.00BC - 34.22A^2 - 12.67B^2 \\ & - 6.67C^2, \end{aligned} \quad (2)$$

$$\begin{aligned} \text{Removal \% of CEF} = & + 93.00 - 7.88A + 1.38B \\ & + 10.75C + 4.50AB - 5.75AC \\ & + 6.25BC - 34.50A^2 - 12.50B^2 \\ & - 6.25C^2, \end{aligned} \quad (3)$$

where *A* is the pH, *B* is the dose of g-C₃N₄ in g L⁻¹ and *C* is the time in minutes. The sign indicates the effect of the variable. A positive sign indicates a direct effect for *B*, *C*, *AB* and *BC*, while a negative sign indicates an inverse effect for *A*, *AC*, *A*², *B*² and *C*².

According to the ANOVA of the model in Table 4, the *F* values were found to be 35.7, 26.4 and 30.5, and the *P* values were found to be 0.0005, 0.0011 and 0.0008 for the removal percentages of LEVO, AZI and CEF, respectively, which implies that the model is significant. The model coefficients (*R*²) were found to be 0.9847, 0.9794 and 0.9821, for the three responses, respectively. This indicates that the quadratic model explained 98.5, 97.9 and 98.2% of the total variances of the three responses. The *R*² and adjusted *R*² values were close to unity, which display the good agreement between experimental and predicted values. The values of the predicted *R*² were found to be in reasonable agreement with the values of the adjusted *R*², which supports the high significance of the model. High adequate precision values (>4) indicate that the model has a high signal-to-noise ratio as shown in Table 4.

The *P* and *F* values were calculated for each independent variable and its interaction. The calculated *F* value of the square term of pH had the largest effect on the removal percentages of the three drugs, followed by the effect of time. However, the dose of nanoparticles showed the minimum effect for the removal of the three drugs. Lack of fit was found to be insignificant for the three responses. The ANOVA of the quadratic model is shown in Supplementary Tables S4, S5 and S6.

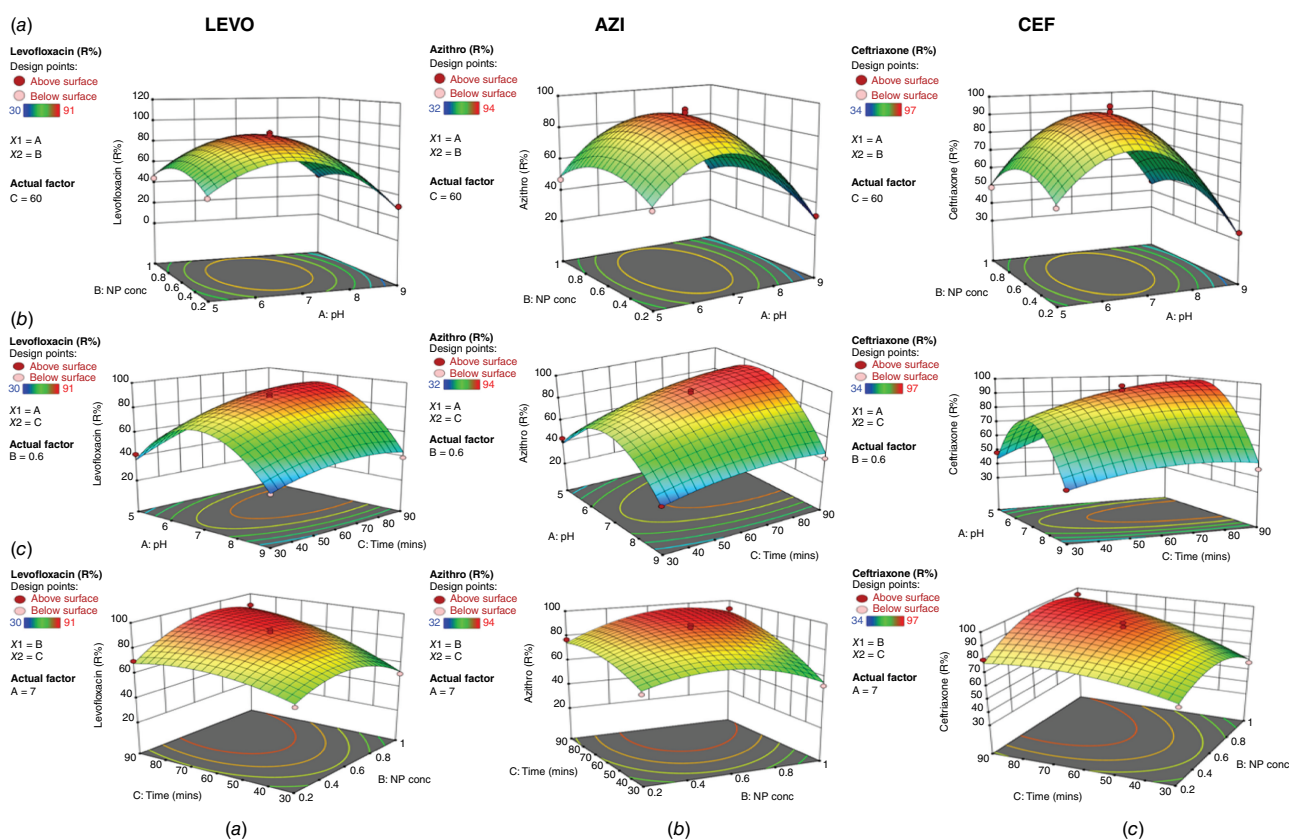


Fig. 4. 3D response surface contour plots showing the simultaneous effects on the removal % of LEVO, AZI and CEF. (a) Effects of pH and the dose of nanoparticles; (b) response surface contour plots showing the effects of pH and time; (c) response surface contour plots showing the effects of time and dose of nanoparticles.

Table 5. Optimisation parameters for removal % of LEVO, AZI and CEF.

Parameters	Optimised value	Predicted removal %			Observed removal % ^A		
		LEVO	AZI	CEF	LEVO	AZI	CEF
A pH	6.66	94.3	97.3	99.6	92.6	98.5	99.1
B Dose of nanoparticles (g L^{-1})	0.71						
C Time (min)	86.40						
Bias %					0.18	1.20	0.46

^AIn the laboratory distilled water spiked with 500 ng mL^{-1} of each of LEVO, AZI and CEF.

Reciprocal effect of variables on the removal percentages

The simultaneous effect of pH and dose of nanoparticles at constant time is shown in Fig. 4a. The pH of the reaction solution governs the surface charge on the photocatalyst. The surface of the prepared photocatalyst with pH values higher than 6.8 will be saturated by negative charges and at lower pH has a positive charge caused by H^+ protons. Photodegradation efficiency was analysed at different pH values 5, 7 and 9 under visible light irradiation. LEVO and CEF contain a variety of functional groups with strongly acidic (carboxylic/sulfonic) or basic (amine/aminothiazole)

properties, so they will be present in three different ionic forms, mainly depending on the pH. At acidic pH 5, they are positively charged, while AZI will exist as zwitterion in the pH range of 3.5–7.7, which explains the minimum interaction between the drug molecules and particles. The percentage removal of the three drugs LEVO, AZI and CEF increases until it reaches a maximum point at pH 7, where the molecules of the three drugs are uncharged. On this basis, it is preferable to keep the pH neutral to avoid repulsions that may cause lesser adsorption to the catalyst surface, which diminishes photodegradation efficiency (Shandilya *et al.* 2018). By increasing the pH of the solution to 9, AZI, CEF

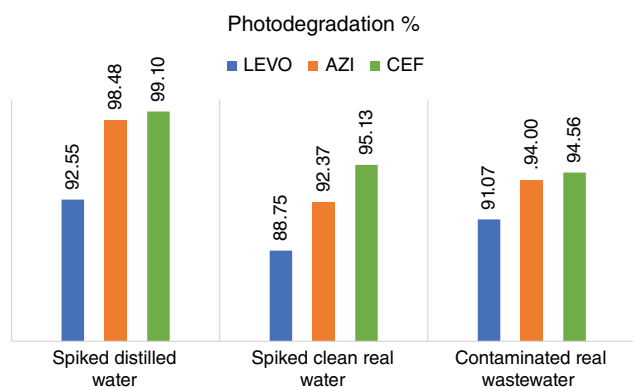


Fig. 5. The calculated average photodegradation % of LEVO, AZI and CEF in spiked distilled water, spiked clean real water and contaminated real wastewater using $g\text{-C}_3\text{N}_4$.

and LEVO molecules acquire a negative charge, which causes repulsion and a decrease in interaction with particles and thus their removal; another factor that can play a major role in low antibiotic degradation is the decomposition of hydroxyl radicals in alkaline media (Fauzi *et al.* 2018).

On the other hand, the removal of the three drugs is maximised at the middle level of the dose of nanoparticles (0.6 g L^{-1}), whereas it slightly decreases at lower and higher doses as shown in Fig. 4a. Additionally, the mutual effect of pH and time at a constant dose of nanoparticles is shown in Fig. 4b, demonstrating that the removal of the three drugs increases with time at pH 7 as mentioned above. The removal % reaches its maximum at 60 min, but no further significant increase is observed against time. Fig. 4c shows the effect of time and dose of nanoparticles at constant pH which shows that the removal of the three drugs is greatly affected by increasing time (from 60 to 90 min) with a lower effect of nanoparticle dose.

Upon applying the optimum conditions, the removal percentage of the studied drugs was maximised as it reached ~97% in only 60 min, so no further modification such as element doping was required to accelerate photocatalytic performance. In addition, the higher surface area of the synthesised $g\text{-C}_3\text{N}_4$ provides more sites for interaction with the studied drugs (Zhu *et al.* 2015).

Optimisation, prediction and model validation

The validation of the RSM model was performed by measuring triplicate experiments in selected optimisation conditions as shown in Supplementary Fig. S6, where the optimised parameters obtained from the statistical analysis showing the highest desirability index (0.886) are listed in Table 5. By comparing actual percentage removal versus predicted percentage removal in the laboratory distilled water spiked with 500 ng mL^{-1} of each of LEVO, AZI and CEF, an error of 0.18, 1.2 and 0.46% was observed for the removal of each drug, respectively. Thus, the second-order polynomial regression equation was confirmed as an

estimate of the accurate percentage of the removal from water samples.

Photodegradation and matrix effect of spiked and real water samples

The optimised conditions were applied to clean real water and compared to the results of the laboratory distilled water samples (both spiked with equal amounts of the three cited pharmaceuticals, 500 ng mL^{-1}), and it was observed that the efficiency of photodegradation in real samples showed a slight decrease than that in distilled water, due to the matrix effect of environmental parameters such as the presence of pollutants other than our studied drug or micro-organisms that might affect their removal, as shown in Fig. 5. The photodegradation of AZI showed the highest matrix effect of 6.20%, while LEVO and CEF showed similar matrix effects of 4.11 and 4.01%, respectively.

Due to the high efficiency of the process by $g\text{-C}_3\text{N}_4$ (>90%) and the low matrix effect for all drugs, the proposed photodegradation procedure was applied to real water samples containing the three cited drugs as shown in Fig. 5. The results of the analysis after photodegradation with $g\text{-C}_3\text{N}_4$ using the adopted chromatographic method are shown in Table 3, where the obtained results were found to be similar to the results of the clean real water samples.

Greenness and whiteness assessments

ComplexGAPI greenness tool

Complex green analytical procedure index (ComplexGAPI) was chosen for the assessment as it provides an evaluation of the entire methodology in addition to the synthesis of the proposed $g\text{-C}_3\text{N}_4$ particles. ComplexGAPI is considered a complementary tool to the previously developed GAPI metric (Płotka-Wasyłka 2018; Płotka-Wasyłka and Wojnowski 2021; Saleh *et al.* 2023). One hexagonal field was added to the original GAPI graph which evaluates several components of the pre-analysis processes and its conditions, the number of rules correlated to green economy, health and safety hazards of chemicals and instrumentation used in the synthesis process, purity of the end products, and calculation of its *E* factor. The original five pictograms of the GAPI tool are subdivided into smaller sub-pictograms to assess 15 aspects related to the analytical method including the type of method, the sample (collection – preservation – transport – storage – preparation), reagents, instrumentation and waste treatment (El-Naem and Saleh 2021; Kayali *et al.* 2023; Mannaa *et al.* 2023).

The ComplexGAPI showed a green profile as it scored 2 red sub-hexagons only related to the high temperature applied during synthesis of $g\text{-C}_3\text{N}_4$ which consumes a high amount energy. Only two red sub-pictograms were scored due to the high energy output of the analytical method (LC-MS/MS) and the non-treated waste of acetonitrile and

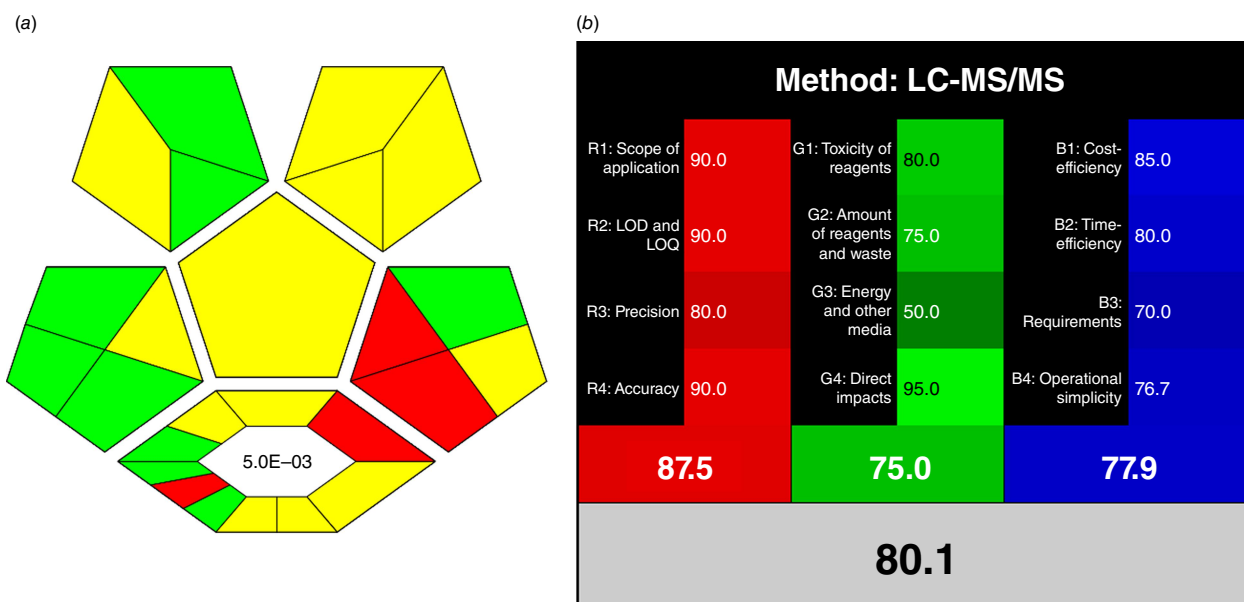


Fig. 6. (a) ComplexGAPI metrics (greenness tool) and (b) RGB 12 algorithms (whiteness tool) for the proposed method.

formic acid with an NFPA score 2 or 3, produced from the method. Applying extraction using Oasis Prime HLB cartridges scored a yellow pictogram due to lower solvent consumption (10–100 mL) and miniaturised procedure. Moreover, the *E* factor was less than 0.1 because the analysis was conducted without any prior preparation, confirming the recommended method's overall environmental friendliness as shown in Fig. 6a. The scores of the pictograms and hexagon are shown in Supplementary Table S7.

RGB 12 algorithms

Analytical procedures are considered sustainable when they consider not just their environmental impact but also their economic cost, validity and efficiency. An effective tool for assessing the sustainability of analytical techniques is the RGB 12 algorithm (Morgan *et al.* 2023). According to White Analytical Chemistry (WAC), RGB 12 includes three principles (red, green and blue) of assessment. Each principle was subdivided into four parameters, for example red is subdivided into R1, R2, R3 and R4, where a score from 0–100 is assigned to each parameter, with 0 being the worst, and 100 means that the method is adapted to this parameter. The red principle (R1–R4), green principle (G1–G4) and blue principle (B1–B4) relate to analytical performance, environmental impact and economic criteria, respectively. The general accordance of the method with all three principles is expressed by an overall quantitative principle known as 'whiteness' (Nowak *et al.* 2021; Elbalkiny *et al.* 2022; Marzouk *et al.* 2023).

The proposed method showed an excellent balance between the three aspects of WAC, scoring an average white score of 80.1 as shown in Fig. 6b. It is worth

mentioning that, through the performed WAC evaluation, all colours and principles were equally important, to maintain the idea of sustainability. This reflects the method's high analytical efficiency, green profile and effective cost.

Conclusion

This study presented a simple, effective method to detect and quantify the repurposed antibiotics LEVO, AZI and CEF in different water samples coinciding with their reported treatment of COVID-19 infections which has led to their extensive use and disposal over the past few years. The quantitation was achieved using LC-MS/MS with positive ion mode for MRM detection. The water samples were extracted by SPE using Oasis HLB Prime cartridges which is considered a green option as it reduces sample preparation time and solvent consumption. This study also described the synthesis and characterisation of a modified green and safe photocatalyst $g\text{-C}_3\text{N}_4$ with increased surface area, and thus higher photocatalytic activity with no need for its doping. The $g\text{-C}_3\text{N}_4$ was used for the photocatalytic degradation of the three drugs of interest from spiked and real water samples under experimental conditions optimised by response surface methodology through Box–Behnken design. The whole procedure was assessed for its greenness and whiteness.

Supplementary material

Supplementary material is available [online](#).

References

- Abdullah M, Iqbal J, Ur Rehman MS, Khalid U, Mateen F, Arshad SN, Al-Sehemi AG, Algarni H, Al-Hartomy OA, Fazal T (2023) Removal of ceftriaxone sodium antibiotic from pharmaceutical wastewater using an activated carbon based TiO₂ composite: adsorption and photocatalytic degradation evaluation. *Chemosphere* **317**, 137834. doi:10.1016/j.chemosphere.2023.137834
- Alias NH, Jaafar J, Samitsu S, Ismail AF, Mohamed MA, Othman MHD, Rahman MA, Othman NH, Nor NAM, Yusof N, Aziz F (2020) Mechanistic insight of the formation of visible-light responsive nanosheet graphitic carbon nitride embedded polyacrylonitrile nanofibres for wastewater treatment. *Journal of Water Process Engineering* **33**, 101015. doi:10.1016/j.jwpe.2019.101015
- Ameen F, Mostafazadeh R, Hamidian Y, Erk N, Sanati AL, Karaman C, Ayati A (2023) Modeling of adsorptive removal of azithromycin from aquatic media by CoFe₂O₄/NiO anchored microalgae-derived nitrogen-doped porous activated carbon adsorbent and colorimetric quantifying of azithromycin in pharmaceutical products. *Chemosphere* **329**, 138635. doi:10.1016/j.chemosphere.2023.138635
- AttariKhasraghi N, Zare K, Mehrzad A, Modirshahla N, Behnajady MA (2021) Achieving the enhanced photocatalytic degradation of ceftriaxone sodium using CdS-g-C₃N₄ nanocomposite under visible light irradiation: RSM modeling and optimization. *Journal of Inorganic and Organometallic Polymers and Materials* **31**, 3164–3174. doi:10.1007/s10904-021-01967-6
- Aydin S, Aydin ME, Ulvi A, Kilic H (2019) Antibiotics in hospital effluents: occurrence, contribution to urban wastewater, removal in a wastewater treatment plant, and environmental risk assessment. *Environmental Science and Pollution Research* **26**, 544–558. doi:10.1007/s11356-018-3563-0
- Balarak D, Mahvi AH, Shahbaksh S, Wahab MA, Abdala A (2021) Adsorptive Removal of Azithromycin Antibiotic from Aqueous Solution by Azolla Filiculoides-Based Activated Porous Carbon. *Nanomaterials (Basel)* **11**, 3281. doi:10.3390/nano11123281
- British Pharmacopoeia Commission (2013) Medicinal & Pharmaceutical Substances. In 'British Pharmacopoeia. Vol I & II'. (Stationary Office: London, UK)
- de Ilurdoz MS, Sathwani JJ, Rebozo JV (2022) Antibiotic removal processes from water & wastewater for the protection of the aquatic environment – a review. *Journal of Water Process Engineering* **45**, 102474.
- Dewil R, Mantzavinos D, Poulios I, Rodrigo MA (2017) New perspectives for Advanced Oxidation Processes. *Journal of Environmental Management* **195**, 93–99. doi:10.1016/j.jenvman.2017.04.010
- Diwan V, Stålsby Lundborg C, Tamhankar AJ (2013) Seasonal and temporal variation in release of antibiotics in hospital wastewater: estimation using continuous and grab sampling. *PLoS One* **8**, e68715. doi:10.1371/journal.pone.0068715
- Dong J, Zhang Y, Hussain MI, Zhou W, Chen Y, Wang L-N (2022) g-C₃N₄: Properties, Pore Modifications, and Photocatalytic Applications. *Nanomaterials* **12**, 121. doi:10.3390/nano12010121
- Elbalkiny HT, El-Zeiny MB, Saleh SS (2022) Analysis of commonly prescribed analgesics using *in-silico* processing of spectroscopic signals: application to surface water and industrial effluents, and comparative study via green and white assessments. *Environmental Chemistry* **19**, 446–459. doi:10.1071/EN22108
- El-Borady OM, Fawzy M, Hosny M (2021) Antioxidant, anticancer and enhanced photocatalytic potentials of gold nanoparticles biosynthesized by common reed leaf extract. *Applied Nanoscience* **13**, 3149–3160. doi:10.1007/s13204-021-01776-w
- El-Maraghy CM, El-Borady OM, El-Naem OA (2020) Effective Removal of Levofloxacin from Pharmaceutical Wastewater Using Synthesized Zinc Oxid, Graphene Oxid Nanoparticles Compared with their Combination. *Scientific Reports* **10**, 5914. doi:10.1038/s41598-020-61742-4
- El-Maraghy CM, Saleh SS, Ibrahim MS, El-Naem OA (2023) Green wastewater treatment of repurposed COVID-19 therapy (levofloxacin) using synthesized magnetite pectin nanoparticles, comparison with mesoporous silica nanoparticles. *BMC Chemistry* **17**, 134. doi:10.1186/s13065-023-01048-4
- El-Naem OA, Saleh SS (2021) Eco-friendly UPLC-MS/MS analysis of possible add-on therapy for COVID-19 in human plasma: insights of greenness assessment. *Microchemical Journal* **166**, 106234. doi:10.1016/j.microc.2021.106234
- Elbalkiny HT, Yehia AM (2022) Artificial networks for spectral resolution of antibiotic residues in bovine milk; solidification of floating organic droplet in dispersive liquid-liquid microextraction for sample treatment. *Spectrochimica Acta Part A: Molecular and Biomolecular Spectroscopy* **266**, 120449. doi:10.1016/j.saa.2021.120449
- Elbalkiny HT, Yehia AM, Riad SM, Elshaharty YS (2019) Removal and tracing of cephalosporins in industrial wastewater by SPE-HPLC: optimization of adsorption kinetics on mesoporous silica nanoparticles. *Journal of Analytical Science and Technology* **10**, 21. doi:10.1186/s40543-019-0180-6
- Elbalkiny HT, Yehia AM, Riad SM, Elshaharty YS (2020) Derivative constant wavelength synchronous fluorescence spectrometry for the simultaneous detection of cefadroxil and cefadroxil in water samples. *Spectrochimica Acta Part A: Molecular and Biomolecular Spectroscopy* **229**, 117903. doi:10.1016/j.saa.2019.117903
- Fauzi AA, Jalil AA, Mohamed M, Triwahyono S, Jusoh NWC, Rahman AFA, Aziz FFA, Hassan NS, Khusnun NF, Tanaka H (2018) Altering fiber density of cockscomb-like fibrous silica-titania catalysts for enhanced photodegradation of ibuprofen. *Journal of Environmental Management* **227**, 34–43. doi:10.1016/j.jenvman.2018.08.073
- Felis E, Kalka J, Sochacki A, Kowalska K, Bajkacz S, Harnisz M, Korzeniewska E (2020) Antimicrobial pharmaceuticals in the aquatic environment-occurrence and environmental implications. *European Journal of Pharmacology* **866**, 172813. doi:10.1016/j.ejphar.2019.172813
- Gao J, Cui Y, Tao Y, Huang L, Peng D, Xie S, Wang X, Liu Z, Chen D, Yuan Z (2016) Multiclass method for the quantification of 92 veterinary antimicrobial drugs in livestock excreta, wastewater, and surface water by liquid chromatography with tandem mass spectrometry. *Journal of Separation Science* **39**, 4086–4095. doi:10.1002/jssc.201600531
- Giacomelli A, Ridolfo AL, Oreni L, Vimercati S, Albrecht M, Cattaneo D, Rimoldi SG, Rizzardini G, Galli M, Antinori S (2021) Consumption of antibiotics at an Italian university hospital during the early months of the COVID-19 pandemic: were all antibiotic prescriptions appropriate? *Pharmacological Research* **164**, 105403. doi:10.1016/j.phrs.2020.105403
- Golovko O, Kumar V, Fedorova G, Randak T, Grabic R (2014) Seasonal changes in antibiotics, antidepressants/psychiatric drugs, antihistamines and lipid regulators in a wastewater treatment plant. *Chemosphere* **111**, 418–426. doi:10.1016/j.chemosphere.2014.03.132
- Gopal G, Natarajan C, Mukherjee A (2022) Adsorptive removal of fluoroquinolone antibiotics using green synthesized and highly efficient Fe clay cellulose-acrylamide beads. *Environmental Technology & Innovation* **28**, 102783. doi:10.1016/j.eti.2022.102783
- Goulart LA, Moratalla A, Lanza MRV, Saez C, Rodrigo MA (2021) Photocatalytic performance of Ti/MMO/ZnO at degradation of levofloxacin: effect of pH and chloride anions. *Journal of Electroanalytical Chemistry* **880**, 114894. doi:10.1016/j.jelechem.2020.114894
- Gulen B, Demircivi P, Simsek EB (2021) UV-A light irradiated photocatalytic performance of hydrothermally obtained W doped BaZrO₃ catalyst against the degradation of levofloxacin and tetracycline antibiotic. *Journal of Photochemistry & Photobiology, A: Chemistry* **404**, 112869. doi:10.1016/j.jphotochem.2020.112869
- Guo X, Li D, Wan J, Yu X (2015) Preparation and electrochemical property of TiO₂/Nano-graphite composite anode for electrocatalytic degradation of ceftriaxone sodium. *Electrochimica Acta* **180**, 957–964. doi:10.1016/j.electacta.2015.09.055
- Guo Y, Chen C, Ling L, Wang J, Qi H, Zhang B, Wu M (2021) Visible-light-driven photo-Fenton degradation of ceftriaxone sodium using SnS₂/LaFeO₃ composite photocatalysts. *New Journal of Chemistry* **45**, 18933–18946. doi:10.1039/D1NJ03639D
- Hashemi SY, Badi MY, Pasalari H, Azari A, Arfaeinia H, Kiani A (2020) Degradation of Ceftriaxone from aquatic solution using a heterogeneous and reusable O₃/UV/Fe₃O₄@TiO₂ systems: operational factors, kinetics and mineralisation. *International Journal of Environmental Analytical Chemistry* **18**, 6904–6920. doi:10.1080/03067319.2020.1817909
- Hayden KR, Jones M, Elkin KR, Shreve MJ, Clees WI, Clark S, Mashtare ML, Veith TL, Elliott HA, Watson JE, Silverman J, Richard TL, Read AF, Preisdanz HE (2022) Impacts of the COVID-19 pandemic on pharmaceuticals in wastewater treated for beneficial reuse: two case studies in central Pennsylvania. *Journal of Environmental Quality* **51**, 1066–1082. doi:10.1002/jeq2.20398

- Hu Z, Ge M, Guo C (2021) Efficient removal of levofloxacin from different water matrices via simultaneous adsorption and photocatalysis using a magnetic $\text{Ag}_3\text{PO}_4/\text{rGO}/\text{CoFe}_2\text{O}_4$ catalyst. *Chemosphere* **268**, 128834. doi:10.1016/j.chemosphere.2020.128834
- ICH Harmonised Tripartite Guideline (2005) Validation of Analytical Procedures: Text and Methodology Q2(R1). (International Conference of Harmonisation, Geneva, Switzerland). Available at <https://database.ich.org/sites/default/files/Q2%28R1%29%20Guideline.pdf>
- Jiang L, Wang Y, Feng C (2012) Application of Photocatalytic Technology in Environmental Safety. *Procedia Engineering* **45**, 993–997. doi:10.1016/j.proeng.2012.08.271
- John A, Thomas J (2022) Enhancement of photocatalytic activity of $\text{g-C}_3\text{N}_4$ under solar light by Nd^{3+} doping and HPA incorporation and its application in the degradation of ceftriaxone sodium. *International Journal of Environmental Analytical Chemistry* 1–25. doi:10.1080/03067319.2022.2036736
- Karampela I, Dalamaga M (2020) Could Respiratory Fluoroquinolones, Levofloxacin and Moxifloxacin, Prove to be Beneficial as an Adjunct Treatment in COVID-19? *Archives of Medical Research* **51**, 741–742. doi:10.1016/j.arcmed.2020.06.004
- Karungamey P, Rugaika A, Mtei K, Machunda R (2022) A Review of Methods for Removal of Ceftriaxone from Wastewater. *Journal of Xenobiotics* **12**, 223–235. doi:10.3390/jox12030017
- Kayali Z, Obaydo RH, Alhaj Sakur A (2023) Spider diagram and sustainability evaluation of UV-methods strategy for quantification of aspirin and sildenafil citrate in the presence of salicylic acid in their bulk and formulation. *Heliyon* **9**, e15260. doi:10.1016/j.heliyon.2023.e15260
- Li C, Jin H, Hou Z, Guo Y (2020a) Study on Degradation of Azithromycin Antibiotics by Molybdenum Sulfide Graphene Oxide Composites under Visible Light. *IOP Conference Series: Materials Science and Engineering* **174**, 012019. doi:10.1088/1757-899X/774/1/012019
- Li J, Tao J, Ma C, Yang J, Gu T, Liu J (2020b) Carboxylated cellulose nanofiber/montmorillonite nanocomposite for the removal of levofloxacin hydrochloride antibiotic from aqueous solutions. *RSC Advances* **10**, 42038–42053. doi:10.1039/D0RA08987G
- Liu R, Yang W, He G, Zheng W, Li M, Tao W, Tian M (2020) Ag-modified $\text{g-C}_3\text{N}_4$ prepared by a one-step calcination method for enhanced catalytic efficiency and stability. *ACS Omega* **5**, 19615–19624. doi:10.1021/acsomega.0c02161
- Mannaa IM, El Gazayerly ON, Abdelbary AA, Saleh SS, Mostafa DA (2023) Validated green spectroscopic manipulation of area under the curve (AUC) for estimation of Simvastatin: application to nanostructured lipid carriers and niosomal systems. *Journal of Research in Pharmacy* **27**, 30–42. doi:10.29228/jrp.285
- Marzouk HM, El-Hanboushy S, Obaydo RH, Fayed YM, Abdelkawy M, Lotfy HM (2023) Sustainable chromatographic quantitation of multi-antihypertensive medications: application on diverse combinations containing hydrochlorothiazide along with LC–MS/MS profiling of potential impurities: greenness and whiteness evaluation. *BMC Chemistry* **17**, 101. doi:10.1186/s13065-023-01015-z
- Mehrdoust A, Jalilzadeh Yengejeh R, Mohammadi MK, Babaei AA, Haghghatizadeh A (2021) Comparative Analysis of UV-assisted Removal of Azithromycin and Cefixime from Aqueous Solution Using PAC/Fe/Si/Zn Nanocomposite. *Journal of Health Sciences & Surveillance System* **9**, 39–49. doi:10.30476/jhss.2020.88564.1149
- Mohammadi Nezhad A, Talaiekhazani A, Mojiri A, Sonne C, Cho J, Rezaia S, Vasseghian Y (2023) Photocatalytic removal of ceftriaxone from wastewater using TiO_2/MgO under ultraviolet radiation. *Environmental Research* **229**, 115915. doi:10.1016/j.envres.2023.115915
- Morgan EM, Lotfy HM, Obaydo RH, Fayed YM, Abdelkawy M, Boltia SA (2023) Whiteness and greenness assessment with efficacy evaluation of two UPLC systems applied for the quantification of cinnarizine and dimenhydrinate along with their toxic impurities. *Sustainable Chemistry and Pharmacy* **36**, 101225. doi:10.1016/j.scp.2023.101225
- Naraginti S, Yu Y-Y, Fang Z, Yong Y-C (2019) Visible light degradation of macrolide antibiotic azithromycin by novel $\text{ZrO}_2/\text{Ag}@\text{TiO}_2$ nanorod composite: transformation pathways and toxicity evaluation. *Process Safety and Environmental Protection* **125**, 39–49. doi:10.1016/j.psep.2019.02.031
- Nowak PM, Wietecha-Posłuszny R, Pawliszyn J (2021) White Analytical Chemistry: an approach to reconcile the principles of Green Analytical Chemistry and functionality. *TrAC Trends in Analytical Chemistry* **138**, 116223. doi:10.1016/j.trac.2021.116223
- Ong W-J, Tan L-L, Ng YH, Yong S-T, Chai S-P (2016) Graphitic carbon nitride ($\text{g-C}_3\text{N}_4$)-based photocatalysts for artificial photosynthesis and environmental remediation: are we a step closer to achieving sustainability? *Chemical Reviews* **116**, 7159–7329. doi:10.1021/acs.chemrev.6b00075
- Opriş O, Soran M-L, Coman V, Copaciu F, Ristoiu D (2013) Determination of some frequently used antibiotics in waste waters using solid phase extraction followed by high performance liquid chromatography with diode array and mass spectrometry detection. *Central European Journal of Chemistry* **11**, 1343–1351. doi:10.2478/s11532-013-0263-y
- Parnham MJ, Erakovic Haber V, Giamarellos-Bourboulis EJ, Perletti G, Verleden GM, Vos R (2014) Azithromycin: mechanisms of action and their relevance for clinical applications. *Pharmacology & Therapeutics* **143**, 225–245. doi:10.1016/j.pharmthera.2014.03.003
- Plotka-Wasyłka J (2018) A new tool for the evaluation of the analytical procedure: Green Analytical Procedure Index. *Talanta* **181**, 204–209. doi:10.1016/j.talanta.2018.01.013
- Plotka-Wasyłka J, Wojnowski W (2021) Complementary green analytical procedure index (ComplexGAPI) and software. *Green Chemistry* **23**, 8657–8665. doi:10.1039/D1GC02318G
- Raizada P, Sudhaik A, Singh P, Shandilya P, Thakur P, Jung H (2020) Visible light assisted photodegradation of 2, 4-dinitrophenol using Ag_2CO_3 loaded phosphorus and sulphur co-doped graphitic carbon nitride nanosheets in simulated wastewater. *Arabian Journal of Chemistry* **13**, 3196–3209. doi:10.1016/j.arabj.2018.10.004
- Saleh SS, Lotfy HM, Elbalkiny HT (2023) [In press] An integrated framework to develop an efficient valid green (EVG) HPLC method for the assessment of antimicrobial pollutants with potential threats to human health in aquatic systems. *Environmental Science: Processes & Impacts* doi:10.1039/D3EM00339F
- Salesi S, Nezamzadeh-Ejhi A (2022) Boosted photocatalytic effect of binary $\text{Ag}/\text{Ag}_2\text{WO}_4$ nanocatalyst: characterization and kinetics study towards ceftriaxone photodegradation. *Environmental Science and Pollution Research* **29**, 90191–90206. doi:10.1007/s11356-022-22100-1
- Sayadi MH, Sobhani S, Shekari H (2019) Photocatalytic degradation of azithromycin using $\text{GO}@\text{Fe}_3\text{O}_4/\text{ZnO}/\text{SnO}_2$ nanocomposites. *Journal of Cleaner Production* **232**, 127–136. doi:10.1016/j.jclepro.2019.05.338
- Serra-Compte A, Pikkemaat MG, Elferink A, Almeida D, Diogène J, Campillo JA, Llorca M, Álvarez-Muñoz D, Barceló D, Rodríguez-Mozaz S (2021) Combining an effect-based methodology with chemical analysis for antibiotics determination in wastewater and receiving freshwater and marine environment. *Environmental Pollution* **271**, 116313. doi:10.1016/j.envpol.2020.116313
- Shandilya P, Mittal D, Soni M, Raizada P, Hosseini-Bandegharai A, Saini AK, Singh P (2018) Fabrication of fluorine doped graphene and SmVO_4 based dispersed and adsorptive photocatalyst for abatement of phenolic compounds from water and bacterial disinfection. *Journal of Cleaner Production* **203**, 386–399. doi:10.1016/j.jclepro.2018.08.271
- Sharma G, Pahade P, Durgbanshi A, Carda-Broch S, Peris-Vicente J, Bose D (2022) Application of micellar liquid chromatographic method for rapid screening of ceftriaxone, metronidazole, amoxicillin, amikacin and ciprofloxacin in hospital wastewater from Sagar District, India. *Total Environment Research Themes* **1**, 100003. doi:10.1016/j.totert.2022.100003
- Shen J, Qian L, Huang J, Guo Y, Zhang Z (2021) Enhanced degradation toward Levofloxacin under visible light with S-scheme heterojunction $\text{In}_2\text{O}_3/\text{Ag}_2\text{CO}_3$: Internal electric field, DFT calculation and degradation mechanism. *Separation and Purification Technology* **275**, 119239. doi:10.1016/j.seppur.2021.119239
- Shokri M, Isapour G, Shamsvand S, Kavousi B (2016) Photocatalytic degradation of ceftriaxone in aqueous solutions by immobilized TiO_2 and ZnO nanoparticles: investigating operational parameters. *Journal of Materials and Environmental Science* **7**, 2843–2851.
- Sun Z, Zhou Q, Yang Y, Li L, Yu M, Li H, Li A, Wang X, Jiang Y (2022) Identification and ultrasensitive photoelectrochemical detection of LncNR_040117: a biomarker of recurrent miscarriage and antiphospholipid antibody syndrome in platelet-derived microparticles. *Journal of Nanobiotechnology* **20**, 396. doi:10.1186/s12951-022-01608-1

- Svoboda L, Škuta R, Matějka V, Dvorský R, Matýsek D, Henych J, Mančík P, Praus P (2019) Graphene oxide and graphitic carbon nitride nanocomposites assembled by electrostatic attraction forces: synthesis and characterization. *Materials Chemistry and Physics* **228**, 228–236. doi:10.1016/j.matchemphys.2019.02.077
- Tantawy MA, Yehia AM, Elbalkiny HT (2023) All-solid-state chip utilizing molecular imprinted polymer for erythromycin detection in milk samples: printed circuit board-based potentiometric system. *Microchimica Acta* **190**, 408. doi:10.1007/s00604-023-05959-w
- Thapa B, Pathak SB, Jha N, Sijapati MJ, Shankar PR (2022) Antibiotics Use in Hospitalised COVID-19 Patients in a Tertiary Care Centre: A Descriptive Cross-sectional Study. *Journal of Nepal Medical Association* **60**, 625–630. doi:10.31729/jnma.7394
- Tian X, Shen Z, Han Z, Zhou Y (2019) The effect of extracellular polymeric substances on exogenous highly toxic compounds in biological wastewater treatment: an overview. *Bioresource Technology Reports* **5**, 28–42. doi:10.1016/j.biteb.2018.11.009
- Ullah A, Zahoor M, Alam S, Ullah R, Alqahtani AS, Mahmood HM (2019) Separation of Levofloxacin from Industry Effluents Using Novel Magnetic Nanocomposite and Membranes Hybrid Processes. *BioMed Research International* **2019**, 5276841. doi:10.1155/2019/5276841
- Upoma BP, Yasmin S, Ali Shaikh MA, Jahan T, Haque MA, Moniruzzaman M, Kabir MH (2022) A Fast Adsorption of Azithromycin on Waste-Product-Derived Graphene Oxide Induced by H-Bonding and Electrostatic Interactions. *ACS Omega* **7**, 29655–29665. doi:10.1021/acsomega.2c01919
- Vella K (2015) Commission implementing decision (EU) 2015/495 of 20 March 2015 establishing a watch list of substances for Union-wide monitoring in the field of water policy pursuant to Directive 2008/105/EC of the European Parliament and of the Council (Position statement). *Official Journal of the European Union*.
- Wang C, Mantilla-Calderon D, Xiong Y, Alkahtani M, Bashawri YM, Al Qarni H, Hong P-Y (2022) Investigation of Antibiotic Resistome in Hospital Wastewater during the COVID-19 Pandemic: Is the Initial Phase of the Pandemic Contributing to Antimicrobial Resistance? *Environmental Science & Technology* **56**, 15007–15018. doi:10.1021/acs.est.2c01834
- WHO Coronavirus (COVID-19) (2023) WHO Coronavirus (COVID-19) Dashboard. World Health Organization. Available at <https://covid19.who.int/>
- Yacouba A, Olowo-okere A, Yunusa I (2021) Repurposing of antibiotics for clinical management of COVID-19: a narrative review. *Annals of Clinical Microbiology and Antimicrobials* **20**, 37. doi:10.1186/s12941-021-00444-9
- Yan H (2012) Soft-templating synthesis of mesoporous graphitic carbon nitride with enhanced photocatalytic H₂ evolution under visible light. *Chemical Communications* **48**, 3430–3432. doi:10.1039/c2cc00001f
- Yasojima M, Nakada N, Komori K, Suzuki Y, Tanaka H (2006) Occurrence of levofloxacin, clarithromycin and azithromycin in wastewater treatment plant in Japan. *Water Science and Technology* **53**, 227–233. doi:10.2166/wst.2006.357
- Yehia AM, Elbalkiny HT, Riad SM, Elsharty YS (2019) Chemometrics for resolving spectral data of cephalosporines and tracing their residue in waste water samples. *Spectrochimica Acta Part A: Molecular and Biomolecular Spectroscopy* **219**, 436–443. doi:10.1016/j.saa.2019.04.081
- Younes HA, Mahmoud HM, Abdelrahman MM, Nassar HF (2019) Seasonal occurrence, removal efficiency and associated ecological risk assessment of three antibiotics in a municipal wastewater treatment plant in Egypt. *Environmental Nanotechnology, Monitoring & Management* **12**, 100239. doi:10.1016/j.enmm.2019.100239
- Yu X, Tang X, Zuo J, Zhang M, Chen L, Li Z (2016) Distribution and persistence of cephalosporins in cephalosporin producing wastewater using SPE and UPLC–MS/MS method. *Science of the Total Environment* **569–570**, 23–30. doi:10.1016/j.scitotenv.2016.06.113
- Zhang W, Zhou L, Deng H (2016) Ag modified g-C₃N₄ composites with enhanced visible-light photocatalytic activity for diclofenac degradation. *Journal of Molecular Catalysis A: Chemical* **423**, 270–276. doi:10.1016/j.molcata.2016.07.021
- Zhang X, Zhang Y, Jia X, Zhang N, Xia R, Zhang X, Wang Z, Yu M (2021) In situ fabrication of a novel S-scheme heterojunction photocatalysts Bi₂O₃/P-C₃N₄ to enhance levofloxacin removal from water. *Separation and Purification Technology* **268**, 118691. doi:10.1016/j.seppur.2021.118691
- Zhao Y, Liang X, Shi H, Wang Y, Ren Y, Liu E, Zhang X, Fan J, Hu X (2018) Photocatalytic activity enhanced by synergistic effects of nano-silver and ZnSe quantum dots co-loaded with bulk g-C₃N₄ for Ceftriaxone sodium degradation in aquatic environment. *Chemical Engineering Journal* **353**, 56–68. doi:10.1016/j.cej.2018.07.109
- Zhu B, Xia P, Ho W, Yu J (2015) Isoelectric point and adsorption activity of porous g-C₃N₄. *Applied Surface Science* **344**, 188–195. doi:10.1016/j.apsusc.2015.03.086

Data availability. The data that supports this study will be shared upon reasonable request to the corresponding author.

Conflicts of interest. The authors declare no potential conflicts of interest concerning the research, authorship and/or publication of this article.

Declaration of funding. The authors received no financial support for the research, authorship and/or publication of this article.

Author contributions. All authors contributed to the study conception and design. Material preparation, data collection and analysis were performed by Heba T. Elbalkiny, Ola M. El-Borady, Sarah S. Saleh and Christine M. El-Maraghy. The first draft of the manuscript was written equally by all authors. All authors read and approved the final manuscript.

Author affiliations

^AAnalytical Chemistry Department, Faculty of Pharmacy, October University for Modern Sciences and Arts (MSA), 11787 6th October City, Cairo, Egypt.

^BInstitute of Nanoscience and Nanotechnology, Kafrelsheikh University, 33516, Kafr ElSheikh, Egypt.